PART *I*

# *PRINCIPLES AND THEORETICAL ASPECTS OF ACCURATE MASS*

# ACCURATE MASS MEASUREMENTS WITH ORTHOGONAL AXIS TIME-OF-FLIGHT MASS SPECTROMETRY

*John C. Fjeldsted*

Director, Research and Development, LC/MS Division, Agilent Technologies, Inc., Santa Clara, California

**AN APPEALING** attribute of time-of-flight mass spectrometry is its fundamental simplicity. It is easy to conceptualize that for a given population of ions all accelerated to the same energy those with the lightest mass will travel with a greater velocity and reach an end point sooner. Simply recording these arrival times and providing a calibration function converts ion arrival times to mass values and produces a simple spectrum.

From simple beginnings time-of-flight has transformed itself into a very powerful analytical tool. The success of orthogonal axis time-of-flight mass spectrometry is the result of both fundamental improvements in analyzer geometry and design as well as technological advances such as those offered by ultra-high-speed signal digitization systems.

This chapter is aimed at giving the practitioner a basic understanding of the underlying theory of TOF mass analysis and instrumental factors critical to achieving the high performance required to meet today's demanding applications.

## 1.1 INTRODUCTION

Since the introduction of commercial orthogonal axis–time-of-flight (oa-TOF) instruments in the mid-1990s, significant improvements have been made to both atmospheric sampling ion sources and TOF mass analysis. Today several manufacturers offer MS and MS/MS instruments which take advantage of oa-TOF's unique combination of speed, sensitivity, resolving power, and mass accuracy. In

combination with a liquid chromatograph oa-TOF is a power tool for the analysis and identification of trace organic substances.

### 1.1.1 History of Time-of-Flight Mass Analysis

The origin of time-of-flight mass spectrometry dates back to 1946 when Stephens presented the concept at the American Physical Society [1] and was first demonstrated by Cameron and Eggers with the analysis of mercury vapor [2]. An important advance in resolving power was achieved by Wiley and McLaren [3] in 1955 with the introduction of space focusing. With additional improvements in ion detection, resolving powers up to 300 where achievable. In 1958 the first commercial TOF instrument was manufactured by Bendix [4]. Due to the high-speed measurement associated with TOF, spectra were recorded with electronic oscilloscopes.

The next critical development needed for TOF was a means of overcoming the effects of initial ion energy spread on flight time. In 1966 Mamyrin, in his doctorate thesis [5], put forth the concept of refocusing ion energy spread which he confirmed by measurement in 1971 [6].

The development of matrix-assisted laser desorption ionization (MALDI) brought a resurgence in TOF mass analysis in the 1980s and 1990s. In contrast to pulsed ionization development, effective coupling to continuous ion sources was first proposed by Dawson and Guilhaus [7, 8] in 1989 and reported by Dodonov et al. in 1991 [9]. The resulting instrumental design is referred to as orthogonal axis time-of-flight mass spectrometry (oa-TOF) and has steadily grown in use due to the wide spread adoption of atmospheric pressure ionization and in particular electrospray ionization. See references [10, 11] for in depth history and instrumental details.

## 1.2 THEORY OF OPERATION

### 1.2.1 Equations for Time-of-Flight

The flight time for each ion of particular *m/z* is unique. The flight time begins when a high-voltage pulse is applied to the back plate of the ion pulser (see Figure 1.1) and ends when the ions of interest strike the detector. The flight time (t) is established by the energy (E) to which an ion is accelerated, the distance (d) it has to travel, and its mass (strictly speaking its mass-to-charge ratio).

There are two well-known formulae that apply to time-of-flight analysis. One is the formula for kinetic energy, the energy of an object (or an ion) in motion, which is expressed as:

$$E = \frac{1}{2} mv^2$$

which solved for m becomes:

$$m = 2E/v^2$$
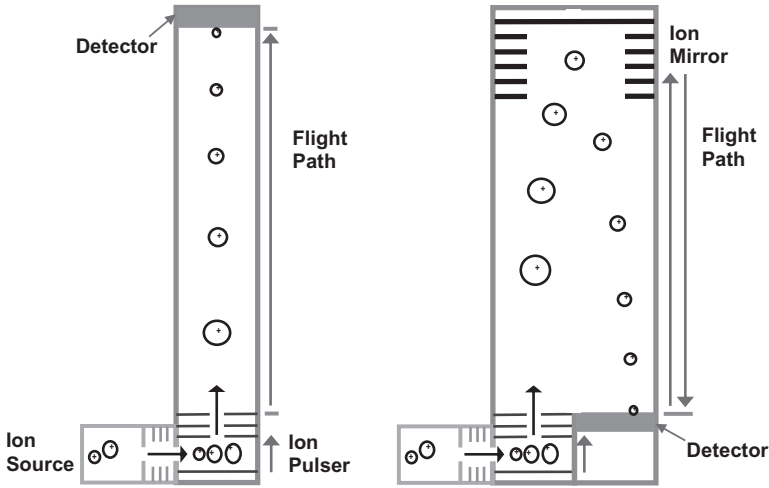
Figure 1.1.    Orthogonal axis time-of-flight mass spectrometers with the configuration on the left showing linear geometry and the configuration on the right incorporating an ion mirror.

The second equation is the familiar equation where velocity (v) equals distance (d) divided by time (t) or:

$$v = d/t$$

Combining the first and second equations yields:

$$m = (2E/d^2)t^2$$

This gives us the basic time-of-flight relationship. For a given energy (E) and distance (d) the mass is proportional to the square of the ion flight time.

The equation stipulates that for a given kinetic energy, E, smaller masses will have larger velocities, and larger masses will have smaller velocities. Hence, ions with lower masses arrive at the detector earlier, as shown in Figure 1.1.

In the design of an oa-TOF mass spectrometer, much effort is devoted to holding the values of the energy (determined by the high voltages) and the distance the ion travels constant, so that an accurate measurement of flight time will give an accurate mass value. As these terms are held constant they are often combined into a single variable, A, so:

$$m = A(t)^2$$

This is an ideal equation, based on true flight times. In practice, there is a delay from the time the control electronics send a start pulse to the time that high voltage is actually present on the ion pulser plates. There is also a delay from the time an ion reaches the front surface of the ion detector until the signal generated by that ion is digitized by the acquisition electronics. These delays are very short, but not insignificant. Because the true flight time cannot be measured, it is necessary to correct the measured time, $t_m$, by subtracting the sum of both the start and stop delay times which, when added together, are referred to as $t_o$.

$$t = t_m - t_o$$

By substitution, the basic formula that can be applied for actual measurements becomes:

$$m = A(t_m - t_o)^2$$

## 1.2.2 Mass Calibration

To make the conversion from measured flight time, $t_m$, to mass, the values of A and $t_o$ must be determined, so a calibration is performed. A mixture of compounds whose exact masses are known with great accuracy is analyzed. Then a simple table (Table 1.1) is established of the flight times and corresponding known masses.

Now that m and $t_m$ are known for a number of values across the mass range, the computer that is receiving data from the instrument does the calculations to determine A and $t_o$. Using an intelligent algorithm, it tries different values of A and $t_o$ until the right side of the calibration equation,

$$m = A(t_m - t_o)^2$$

matches as closely as possible the left side of the equation (m), for all seven of the mass values in the calibration mix.

While this initial determination of A and $t_o$ is highly accurate, it is still not accurate enough to give the best possible mass accuracy for time-of-flight analysis. A second calibration step is needed. After the calibration coefficients A and $t_o$ have been determined, a comparison is made between the actual mass values for the calibration masses and their calculated values from the equation. These typically deviate by only a few parts-per-million (ppm). Because these deviations are small and relatively constant over time, it is possible to perform a second-pass correction to achieve an even better mass calibration. This is done via an equation that corrects the small deviations across the entire mass range. This correction equation (typically a higher-order polynomial function) is stored as part of the instrument calibration. The remaining mass error after this two-step calibration method, neglecting all other instrumental factors, is typically at or below 1 ppm over the range of calibration masses.

**TABLE 1.1. TOF Mass Calibration**

| Calibrant Compound Mass (m) | Flight Time (μsec) ($t_m$) |
| --- | --- |
| 118.0863 | 20.79841 |
| 322.0481 | 33.53829 |
| 622.029 | 46.12659 |
| 922.0098 | 55.88826 |
| 1521.971 | 71.45158 |
| 2121.933 | 84.14302 |
| 2721.895 | 95.13425 |

## 1.2.3   TOF Measurement Cycle

TOF measurements do not rely on the arrival times of ions coming from just a single pulse applied to the ion pulser, but instead are summations of the signals resulting from many pulses. Each time a high voltage is triggered to the plates of the ion pulser, a new spectrum (called a single transient) is recorded by the data acquisition system. This is added to previous transients until a predetermined number of sums have been made. For analyses requiring a scan speed of one spectrum per second, approximately 10,000 transients can be summed before transferring the data from the instrument back to the host computer to be written to disk. If the target application involves high-speed chromatography, then fewer transients are summed and the rate at which spectra are recorded is increased.

The mass range limits the number of times per second that the ion pulser can be triggered and transients recorded. Once the ion pulser fires, it is necessary to wait until the last mass of interest arrives at the ion detector before the ion pulser is triggered again. Otherwise light ions triggered from the second transient would arrive before the heavier ions of the first transient, resulting in overlapping spectra.

Table 1.2 shows several example masses with their approximate flight times and possible transients/second. These are calculated for an effective flight length of 2 meters and an accelerating potential of 6500 volts. Under these conditions, a mass of 3200 has a flight time of about 100 microseconds (μsec). As there is essentially no delay time between transients, this means that 10,000 transients/second correspond to a mass range of 3200 $m/z$. For a smaller mass range, the ion pulser can be triggered at higher rates. For example, a mass range of 800 $m/z$ (one-fourth of 3200 $m/z$) reduces the flight time to 0.1 msec/$\sqrt{4}$, or 0.05 milliseconds, allowing for 20,000 transients/second. Conversely, extending the transient to 0.141 milliseconds doubles the mass range to 6400 $m/z$ (remember, mass is a function of the time squared).

Because each transient takes place in such a short period of time, the number of ions for any particular compound at a specific mass is often quite small and for many oa-TOF instruments traditionally substantially less than one. Historically, this fact plays an important role in the basic design of the data acquisition system of many of today's commercial instruments.

**TABLE 1.2.   Flight Time and Transients/Second as a Function of Mass***

| m/z | Flight Time (μsec) | Transients/sec |
|---|---|---|
| 800 | 50 | 20,000 |
| 3200 | 100 | 10,000 |
| 6400 | 141 | 7070 |

*Two-meter flight effective flight path, flight potential 6500 V.

## 1.3   THE RELATIONSHIP BETWEEN MASS RESOLVING POWER AND MASS ACCURACY

### 1.3.1   Instrumental Limitation to Mass Resolving Power

Even in the case of an ideal mass spectrometer which exhibited perfect ion acceleration and flight distance stability there exists factors that produce variations in the ion arrival time for a given mass. The major source of variation arises from the position and energy each ion possess in the ion pulser at the instant that the high-voltage pulse initiates each transient measurement cycle.

The first of these two potential sources of variation, position in the ion pulser, is largely corrected for using Wiley-McLaren space focusing [3, 12]. Under Wiley-McLaren space focusing, a potential gradient is established across the ion pulser region. With a higher potential at the rear of the pulser region, these ions which have a greater distance to travel also receive a greater acceleration potential. The result is that the ions accelerated from the rear of the ion pulser actually "catch up" with those closer to the front of the pulser and are therefore refocused in time.

The second source for variation in ion arrival time is related to the initial energy of each ion in the ion pulser and is commonly referred to as the "turnaround time." To understand this effect consider two ions of equal mass and both at the same identical position in the ion pulser. The first of these two ions has a small residual energy in line with the field that the pulser applies to accelerate the ions for the time-of-flight measurement. The second has the same small residual energy, but its velocity is directed against the orthogonal accelerating field. At the instant the high-voltage pulser is triggered the first ion accelerates quickly in the desired direction. For a brief moment, the second ion travels in the opposite direction until its initial energy is lost, then re-accelerates past its origin, delayed from the launch of the first ion by a short period of time. The turn around time, $\Delta t$, can be calculated by the expression

$$\Delta t = 2v/a$$

where $v$ is initial ion velocity directed against the desired orthogonal flight path and $a$ is the ion acceleration in pulser field.

There are three principal approaches to minimize the broadening of ion arrival time. The first is to minimize the energy spread of the beam entering the ion pulser. Most instruments take advantage of beam forming optics and slits to minimize beam divergence entering the pulser. For clarification, it is the energy of the ions orthogonal to entry into the pulser (i.e., the axis of the time of flight measurement) that is critical.

The second instrumental factor is to increase the potential applied to the plates that accelerate the ions in the ion pulser thereby increasing the accelerating field. This plays together with the instrumental requirements for Wily-McLaren space focusing. In practice it also creates a rather large spread in ion energy for ions exiting the ion pulser. It is for this reason that all oa-TOF instruments make use of an ion mirror that compensates for this energy spread.

The reflectron or Mamyrin ion mirror [6] is placed at the end of the flight tube where in "linear" instruments the ion detector is positioned. The mirror is constructed with a stacked set of metal rings each having a higher electrical potential applied. Ions penetrate the field established by these rings until they loose all forward energy and their direction of travel is reversed. The greater the energy the ions possess entering the ion mirror, the greater the penetration and resulting distance that is traveled. The potential field in the ion mirror is precisely established so that the time required to travel the additional distance is exactly canceled by the ion's greater ion energy.

The third instrumental factor is to increase the flight time of the measured ions. Because mass is proportional to the square of ion arrival time the mass resolving power is one half the ion arrival time (t) divided by the spread in ion arrival time (Δt), which is principally the ion turnaround time:

$$\text{Mass Resolving Power} = t/(2\Delta t)$$

For a given acceleration potential the ion arrival time, and hence the mass resolving power, is established by the length of the ion flight path. With a 2 meter effective flight path and a corresponding flight time of 50 μsec a turnaround time of 1.67 nsec results in a resolving power of 15,000 using the mass resolving power equation above.

## 1.3.2 The Effect of Ion Detection on Resolving Power

In an ideal instrument the exact arrival time for each ion would be detected and recorded without any effect on the actual ion population being measured. In reality, with high ion currents and an arrival time variation on the order of 1 nsec this becomes very challenging to achieve instrumentally. While detector response times can reach down to the 100s of picoseconds, this is still insufficient with high-sensitivity designs that can present up to 100s of ions within this 1 nsec spread. Under such conditions, detecting individual ion arrival times is not possible. To get around this challenge two different approaches have been developed.

The historical approach for time-of-flight ion arrival detection is based on a Time to Digital Converter (TDC) together with a discriminator to selectively register an arrival when the output of the ion detector crosses a set threshold. This approach was considered important so as to maximize ion detection and reduce electronic noise. The limitation when using such a threshold detection system is that, as sample levels increase, multiple ion arrivals occur for a given mass within a single transient. When such is the case two consequences occur. The first is that the earliest ion to arrive for a given mass triggers the TDC with some of the later part of the distribution being missed. This results in an apparent shift towards lower arrival times and hence a shift towards lower reported mass. As ion intensity continues to increase, individual ions have coinciding arrival times which results in only a single response, thereby truncating the recorded signal. This causes an amplitude saturation effect, and for this reason, oa-TOF has historically not been considered suitable for quantitative analysis.

One approach found in commercial instrumentation to extended dynamic range is through the use of a segmented detector and a multi-input TDC. By reduction of the ion capture area of an individual segment, a higher signal level can be accommodated.

More recently, some instruments that use TDC acquisition systems have incorporated controllable beam attenuator which can be automatically invoked by the instrument acquisition system to decrease the ion transmission before it is pulsed for mass measurement. This results in an increase of dynamic range, but at the cost of losing ion signal which ultimately limits mass accuracy and reduces in-scan dynamic range.

A more recent approach to recording ion arrival time for oa-TOF instruments makes use of high-speed Analog to Digital Converter (ADC) technology. Unlike the discriminator TDC approach, an ADC is able to measure the analog response of the ion detector and can track the ion abundance as it increases. This gives ADC-based systems greater intrinsic dynamic range. The downside for ADC-based systems can be found in the fact that included in the ion arrival measurement is an apparent broadening of the ion arrival distribution. This can be explained when one considers that the analog response of the ion detector has a finite width which gets summed into digitization process.

### 1.3.3   Translating Mass Resolving Power to Mass Accuracy

At this point we have determined a nominal mass resolving power for an oa-TOF mass spectrometer. A resolving power specification of 15,000 is shown for *m/z* 1500 in Figure 1.2. A simple calculation gives us the peak width (FWHM) of this mass peak of 0.10 *m/z*.

If the mass measurement obtained from the mass spectrometer pertains only to that of single ions then the mass accuracy is directly related to the resolving power. As measurement accuracy is generally specified using standard deviation, conver-

$$\mathrm{FWHM} = 2\sqrt{2\ln(2)}\,\sigma \sim 2.35\,\sigma$$
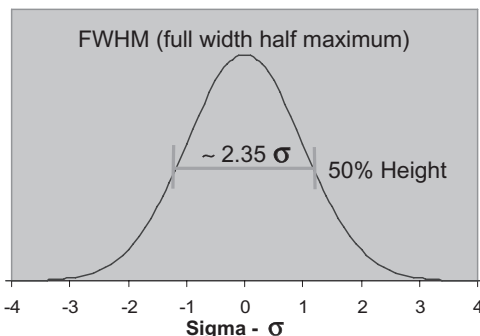


Figure 1.2.    Relationship between FWHM and standard deviation for a normal distribution.

sion between a peak's full width half maximum value and standard deviation is required.

Considering a mass at $m/z$ 1500 and a resolving power of 15,000 the observed FWHM peak width is 0.1 $m/z$. The standard deviation for individual ion arrival ($1\sigma$) is equal to 0.043 $m/z$. It is customary to specify the mass accuracy as a relative unit expressed in parts per million, or in this case 28 ppm ($1\sigma$). As $\pm 1\sigma$ represents only 68.3% of the measurement distribution, $2\sigma$ values representing 95.4% of the measurement distribution are often specified.

Absent from the above calculations of mass measurement accuracy is the consideration that each mass measurement is the summation of a large number of transients and generally a large number of ions which populate the arrival distribution. The relationship between the number of ions contributing to the distribution reduces the uncertainty when establishing the mean. This improvement in mass measurement accuracy follows the central limit theorem according to

$$\sigma_{mean} = \sigma_{single\ event} / \sqrt{n}$$

where n = number of single events included in the mean.

Continuing the previous example, the distribution for a single ion arrival with a resolving power of 15,000 has a $2\sigma$ confidence interval of 56 ppm, the accuracy of assigning the mean is reduced by the square root of the number of ions detected (see Table 1.3).

The number of ions detected in a measurement is dependent on the quantity of analyte and the sensitivity of the mass spectrometer. While mass spectrometers vary in ionization and transmission efficiency, for standard electrospray operation it is estimated that 1 ng of a reasonably well ionizing analyte results in between 10,000 and 100,000 detected ions depending on the instrument. For fragment ions of an MS/MS spectrum this value is typically reduced by the fraction of ions associated in the MS/MS transition of interest. When based solely on resolving power and ion statistics, oa-TOF can achieve 2 ppm mass accuracy with as little as 10 pg when measured with the most sensitive of instruments.

**TABLE 1.3.   Relationship Between Ion Statistics and Theoretical Limit of Mass Measurement Accuracy for a Resolving Power of 15,000**

| Number of Ions Detected | 2 sigma (95% confidence) |
| --- | --- |
| 1 | 56 ppm |
| 10 | 18 ppm |
| 100 | 5.6 ppm |
| 1000 | 1.8 ppm |
| 10,000 | 0.56 ppm |
| 100,000 | 0.18 ppm |

## 1.4 OPERATIONAL FACTORS AND PRACTICAL LIMITS

### 1.4.1 Reference Mass Correction

Achieving an accurate mass calibration is the first step in producing accurate mass measurements. When the goal is to achieve accuracies at the 1 ppm level, even the most miniscule changes in accelerating potentials or flight distances can cause a noticeable shift. It is possible to cancel out these instrumental drift factors with the use of reference mass recalibration. With this technique, compounds of known mass are introduced into the ion source while samples are being analyzed. The presence of reference masses in the acquired spectrum allows calibration corrections to be made on individual or averaged mass spectra. This can be accomplished by the data processing software, or ideally it is performed automatically during the analysis as spectra are initially stored to disk.

### 1.4.2 Mass Assignment Errors Due to Chemical Interferences

The second significant factor that limits mass accuracy is chemical background. The high resolving power of a TOF system helps to reduce the chances of having the peak of interest merged with background, yet even a small unresolved impurity can shift the centroid of the expected mass. The magnitude of this effect can be estimated by using a simple weighted average calculation:

$$\Delta_{obs} = \Delta_{contaminant} \cdot Abd_{contaminant} / (Abd_{contaminant} + Abd_{sample})$$

where

$\Delta_{obs}$ is the observed shift in mass in ppm

$\Delta_{contaminant}$ is the mass difference between the sample and contaminant in ppm

$Abd_{contaminant}$ and $Abd_{sample}$ are the mass peak heights or areas of the contaminant and sample

For a resolving power of 10,000, a mass difference between the sample and contaminant of 50 ppm, and relative mass peak heights of 10 : 1 (sample vs background) the observed mass shift would be 50 · 1 / (1 + 10) or about 5 ppm.

There are a number of ways to minimize chemical background. Of instrumental importance is to use system with a sealed ion source chamber that minimizes contamination from the laboratory air. It is also essential to use high-purity HPLC solvents and follow a systematic cleaning program for the HPLC and the ion source.

### 1.4.3 Enhanced Performance Through Novel Acquisition Systems

The combination of ultra-high-speed sampling and real-time signal processing enables two new modes of operation. They are referred to as Transient Level Peak Picking (TLPP) and simultaneous dual gain mode. In TLPP mode, as each TOF
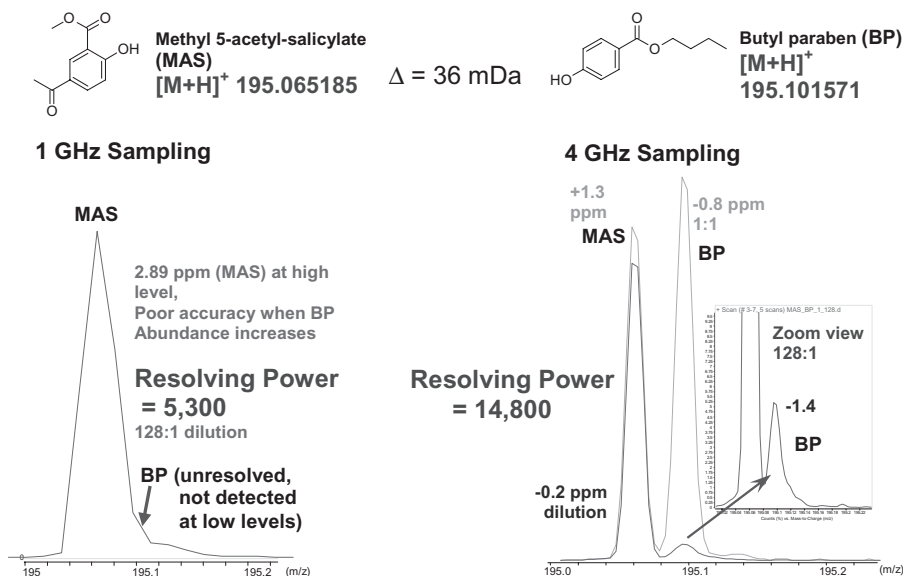
Figure 1.3. Comparison of resolving power achievable with 1 GHz and advanced 4 GHz technology.

transient (a transient is the individual time-of-flight spectrum acquired from each TOF pulse) is acquired the precise arrival time of the ion packet for each mass is determined in real time. This maximizes resolution which is similar to operation with a TDC. What differentiates TLPP from a TDC is that the arrival time of each packet of ions for each mass is triggered at the peak apex instead of the first ion or leading edge of the ion packet. Using apex detection not only is the arrival time recorded, but also the signal intensity. This is only possible with an ADC and dramatically extends the in-spectrum dynamic range. Apex detection also eliminates the need for dead time correction critical to TDC operation.

In dual gain mode the 4 GHz sampling rate is divided into two channels of data acquisition. One channel operates with the standard preamplifier gain. The second channel operates at a reduced gain. Both channels are acquired simultaneously at 2 GHz. In this way there is never a need to attenuate the ion current transferred to the TOF mass spectrometer. Once the desired number of TOF transients has been summed, the standard and reduced gain spectra are merged in such a way that any peaks that saturated the standard gain channel are replaced by the data coming from the reduced gain channel. The advantage of dual gain mode is that all ions are detected, maximizing ion statistics, which improves mass accuracy while simultaneously extending the dynamic range.

With 4 GHz sampling and TLPP higher resolving power is now possible with ADC systems. Figure 1.3 shows how two isobars can now be fully resolved even with a broad spread in concentration.

With dual gain mode, spectra are simultaneously acquired at standard and at low gain levels. Before spectra are sent from the mass spectrometer to the host
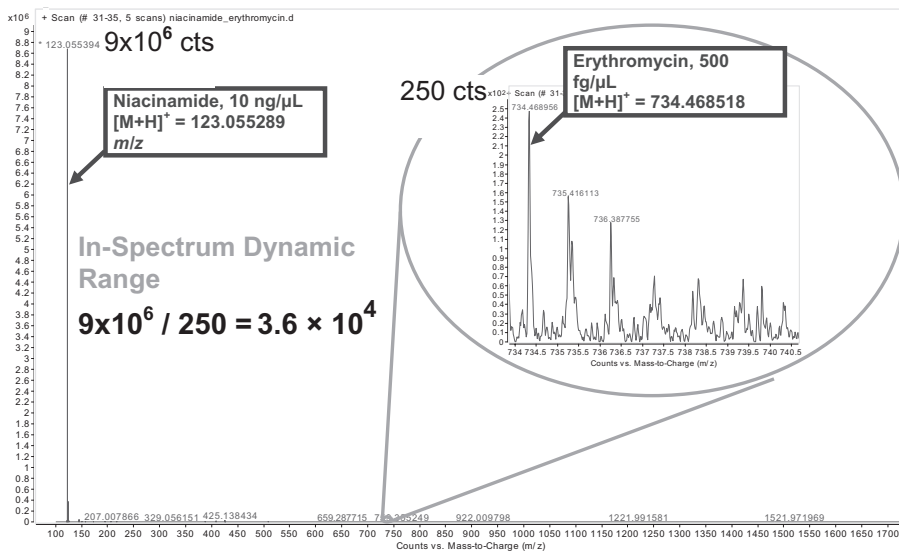
Figure 1.4.   High in-spectrum dynamic range resulting from simultaneous dual gain acquisition.

computer, any mass peaks in the spectrum which are saturated at the standard gain spectrum are replaced with corresponding data points from the low gain spectrum. Figure 1.4 shows the detection of both high and very low level analytes differing in response by 4.5 decades.

## 1.5   CONCLUSIONS

What sets oa-TOF apart from other methods of mass analysis is its unique combination of speed, mass accuracy, sensitivity and dynamic range. Table 1.4 indicates performance achievable on leading instruments. What is unique to TOF is that each of these specifications can be simultaneously achieved when working with significant signal to noise and ion statistics.

As compared to quadrupole mass filter-based mass spectrometers, oa-TOF offers higher mass accuracy, resolving power, full-spectrum sensitivity, and speed, while quadrupole mass filters offer the ultimate in single ion monitoring sensitivity and instrumentation cost.

As compared to 2D and 3D ion trap mass spectrometers, oa-TOF has greater mass accuracy, resolving power, speed, and, with the latest generation acquisition systems, in-spectrum dynamic range. Ion traps on the other hand generally have the highest full scan sensitivity.

While FT-ICR systems demonstrate unsurpassed resolving power at low *m/z* ions and low data acquisition rates, other key performance factors favor TOF. These include in-spectrum dynamic range, speed and cost. When considering mass accu-

TABLE 1.4.  Properties of a High Performance oa-TOF
System

| Property | Specification |
|---|---|
| Mass accuracy | <2 ppm |
| Mass range | >10,000 m/z |
| Resolving power | Up to 20,000 |
| Sensitivity | <10 pg |
| Dynamic range—in spectrum | Up to 5 decades |
| Speed—spectra/sec | Up to 40/sec |
| Cost | Moderate |

racy the difference between nonmagnetic Fourier transform (Orbitrap) and high-performance oa-TOF systems appears to be less than a factor of 2.

Considering the complexity of many current LC/MS applications, oa-TOF offers key analytical value particularly in light of the ability to effectively couple to a high-resolution chromatographic separation system, where high speed, high dynamic range, and very low part-per-million mass accuracy is required.

# REFERENCES

1. Stephens, W.E., A pulsed mass spectrometer with time dispersion, *Phys. Rev.*, **1946**, 69, 691.
2. Cameron, A.E.; Eggers, D.F., An ion "velocitron," *Rev. Sci. Instrum.*, **1948**, 19, 605–607.
3. Wiley, W.C.; McLaren, I.H., Time-of-flight mass spectrometer with improved resolution, *Rev. Sci. Instrum.*, **1955**, 26, 1150–1157.
4. Scripps Center for Mass Spectrometry website, http://masspec.scrips.edu/mshistory/perspectives/timeline.php
5. Mamyrin, B.A., Time-of-flight mass spectrometry (concepts, achievements, and prospects), *Int. J. Mass Spectrom.*, **2001**, 206, 251–266.
6. Karataev, V.I.; Shmikk, D.V.; Mamyrin, B.A., New method for focusing ion bunches in time-of-flight mass spectrometers, *J. Tech. Phys.*, **1972**, 16, 1177–1189.
7. Dawson, J.H.J.; Guilhaus, M., Orthogonal-acceleration time-of flight mass spectrometer, *Rapid Commun. Mass Spectrom.*, **1989**, 3, 155–159.
8. Coles, J.; Guilhaus, M., Orthogonal acceleration—a new direction for time-of-flight mass spectrometry: fast, sensitive mass analysis for continuous ion sources, *Trends Anal. Chem.*, **1993**, 12, 203–213.
9. Dodonov, A.F.; Chernushevich, I.V.; Laiko, V.V., *Proceedings of the 12th International Mass Spectrometry Conference,* 26–30.
10. Igor, V.; Chernushevich, A.; Loboda, V.; Thomson, B.A., An introduction to quadrupole time-of-flight mass spectrometry, *J. Mass Spectrom.*, **2001**, 36, 849–865.
11. Tamura, J.; Osuga, J., Next Generation LC-TOF/MS—AccuTOF, Application Note, JEOL, Ltd., 2001.
12. Seccombe, D.P.; Reddish, T.J., Theoretical study of space focusing in linear time-of-flight mass spectrometers, *Rev. Sci. Instrum.*, **2001**, 72, 1330–1338.